Supplementary Information for

Deforestation triggering irreversible transition in Amazon hydrological cycle

Xiyan Xu[1], Xiaoyan Zhang[2,3], William J. Riley[4], Ying Xue[5], Carlos A. Nobre[6], Thomas E. Lovejoy[7], Gensuo Jia[1*]

[1]Key Laboratory of Regional Climate-Environment for Temperate East Asia, Institute of Atmospheric Physics, Chinese Academy of Sciences, Beijing 100029, China

[2]School of Atmospheric Science, Nanjing University of Information Science and Technology, Nanjing 210044, China

[3]Department of Occupational and Environmental Health, University of Oklahoma Health Sciences Center, University of Oklahoma, Oklahoma City 73104, USA

[4]Climate and Ecosystem Sciences Division, Lawrence Berkeley National Laboratory, Berkeley, California 94720, USA

[5]School of Applied Meteorology, Nanjing University of Information Science and Technology, Nanjing 210044, China

[6]Institute of Advanced Studies, University of São Paulo, São Paulo SP 05508-060, Brazil

[7]Department of Environmental Science and Policy, George Mason University, Fairfax, VA 22030-4444, USA

List of supplementary materials：

Table S1 Number of 0.5-degree gridcells for each forest loss category

	Forest loss	0-5%	5-10%	10-20%	20-30%	>30%
Number of gridcells	Savannas	1065	460	344	119	63
	Seasonal forests	671	139	122	69	28
	Rainforests	996	81	49	18	5

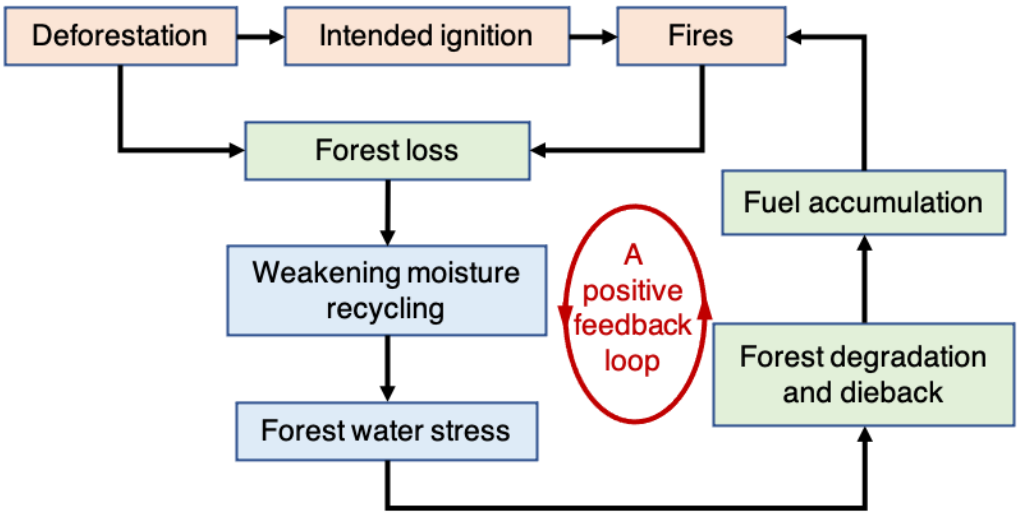

Figure. S1 Illustration of the positive feedback loop among deforestation, fires, forest loss and weakening moisture recycling in Amazonian forests.

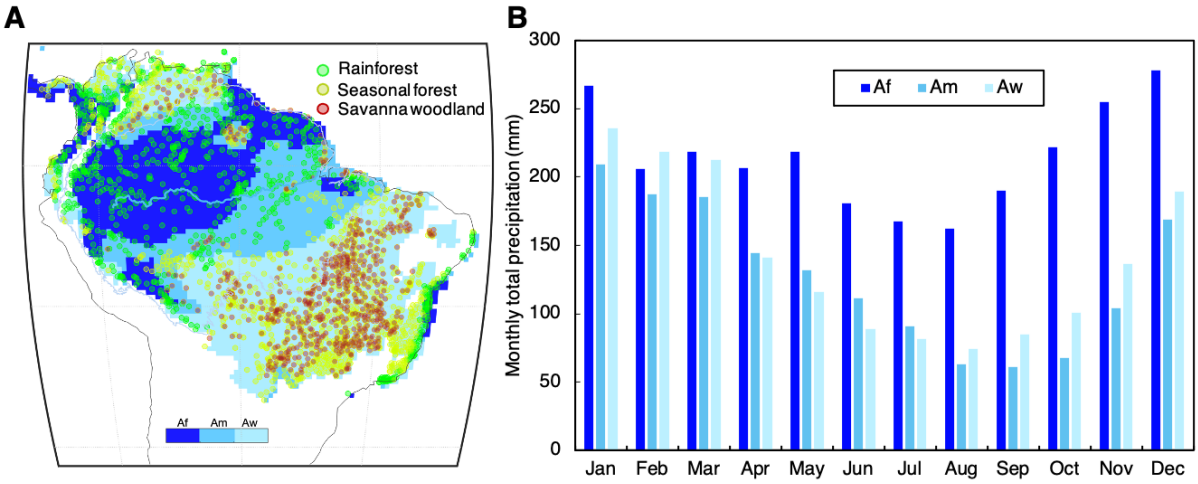

Figure. S2 The Amazonia vegetation, climates and monthly total precipitation distributions. (A) The distribution of tropical rainforest climate (Af) dominated by rainforests, tropical monsoon climate (Am) with a transition from rainforests to seasonal forests and tropical savanna with winter dry climate (Aw) dominated by mixed seasonal forests and savanna woodlands; (B) The monthly total precipitation (mm) averaged over 1961–1990 in rainforests, monsoon forests and savannas.

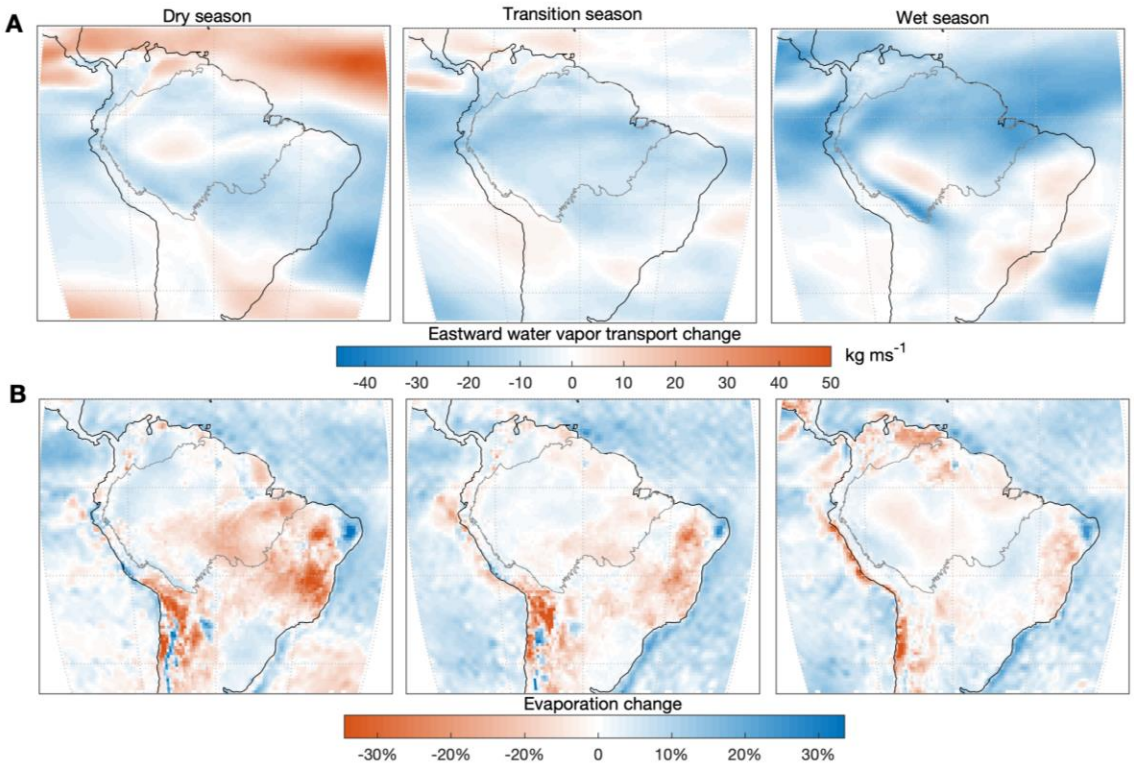

Figure. S3 Changes in vertically integrated eastward water vapor transport and evaporation. (A) Changes in vertically integrated eastward water vapor transport (ΔVT, kg ms^{-1}) and (B) relative changes in surface evaporation (ΔET, %) during 2000–2019 in relative to 1980–1999 for dry, transition and wet seasons.

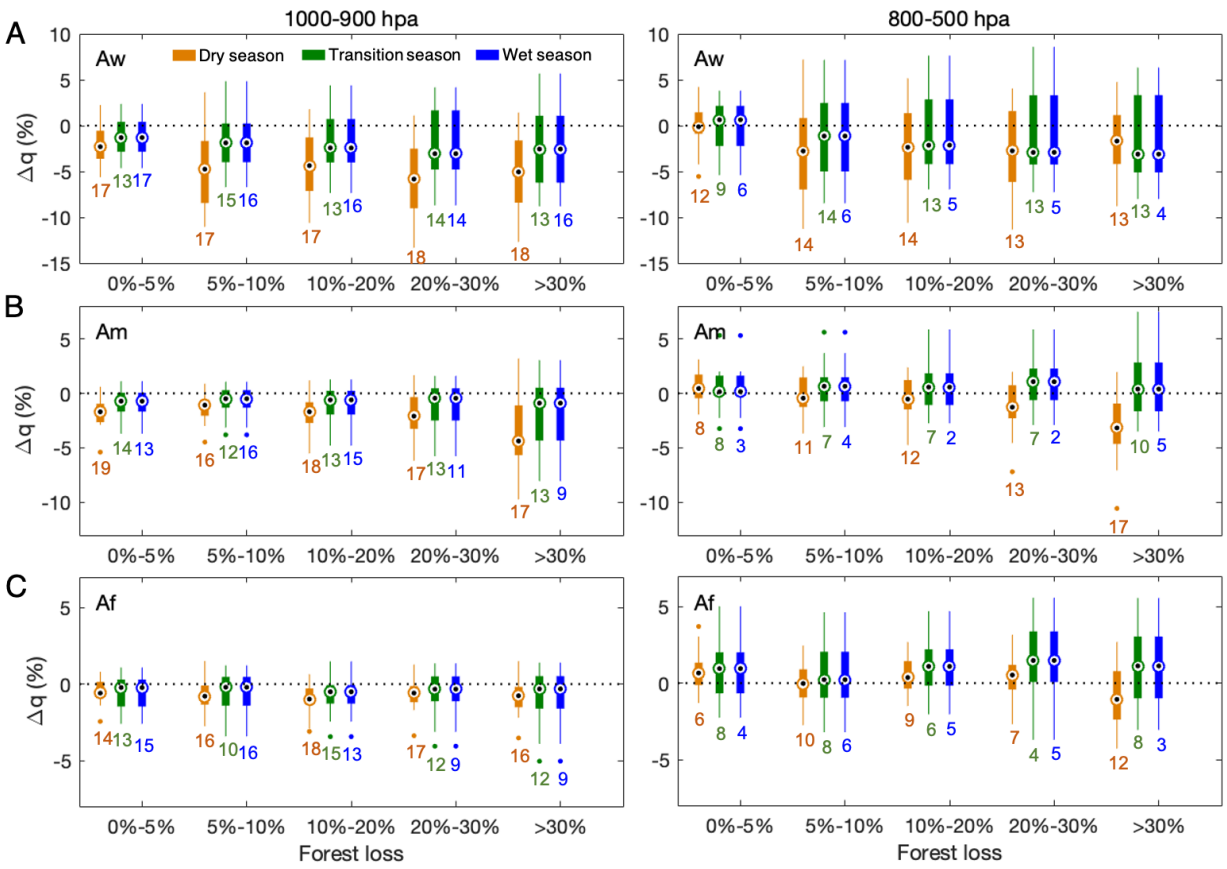

Figure. S4 Relative change of specific humidity as a function of forest loss in lower and middle troposphere. The boxplots of relative change of specific humidity (Δq, %) for each forest loss category over 2000–2019 in relative to 1980–1999 for tropical (A) savanna (Aw), (B) monsoon (Am) and (C) rainforest (Af) climate zones in lower troposphere (1000–900 hpa) and middle troposphere (800–500 hpa)**.** The number under each box indicates the number of years with negative change of specific humidity during 2000–2019 in relative to the mean specific humidity in 1980–1999.

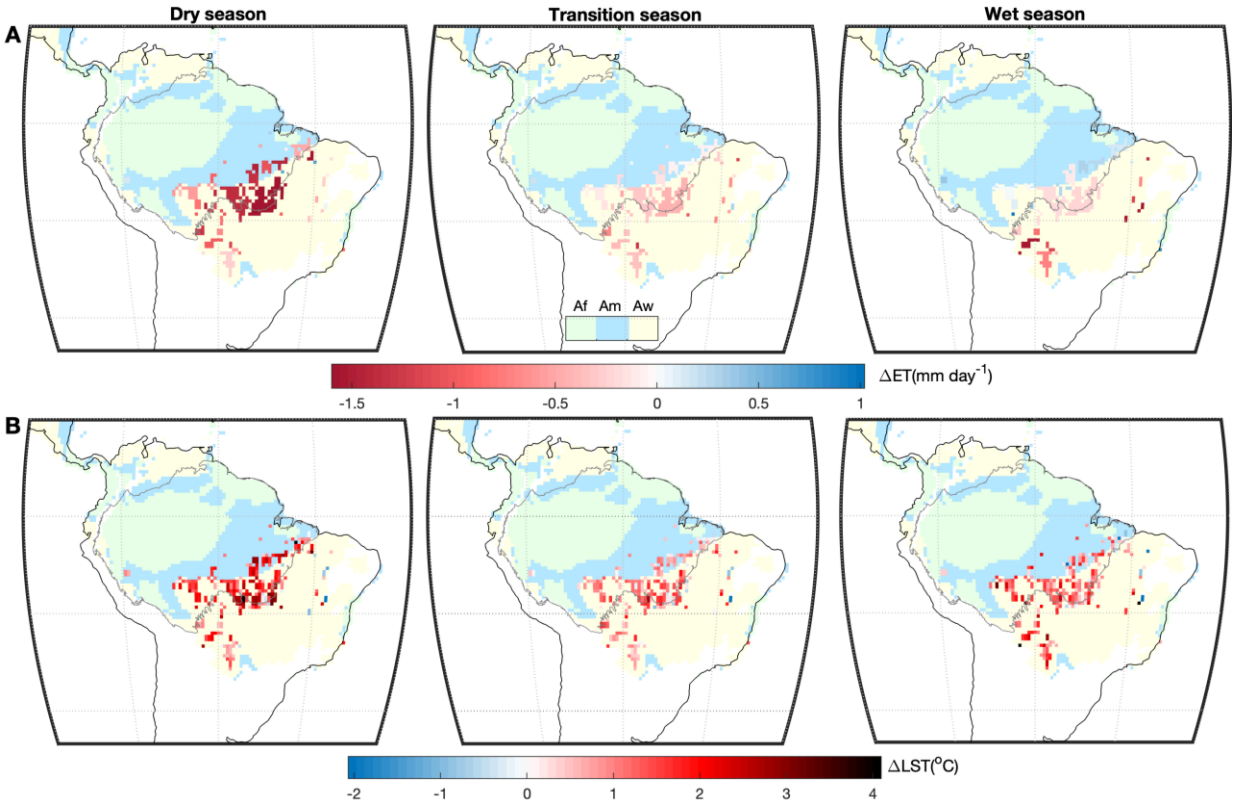

Figure. S5 Deforestation induced anomalies of evapotranspiration and land surface temperature. Satellite observed (A) evapotranspiration (ΔET, mm day^{-1}) and (B) land surface temperature (ΔLST, °C) difference between significantly disturbed forest (forest loss>65%) and intact forest (forest loss<5%) with similar climate background. These maps only display the 0.5-degree gridcells in which forest loss>65% and forest loss<5% coexist. The background colors denote tropical rainforest (Af), monsoon (Am) and savanna (Aw) climate zones.

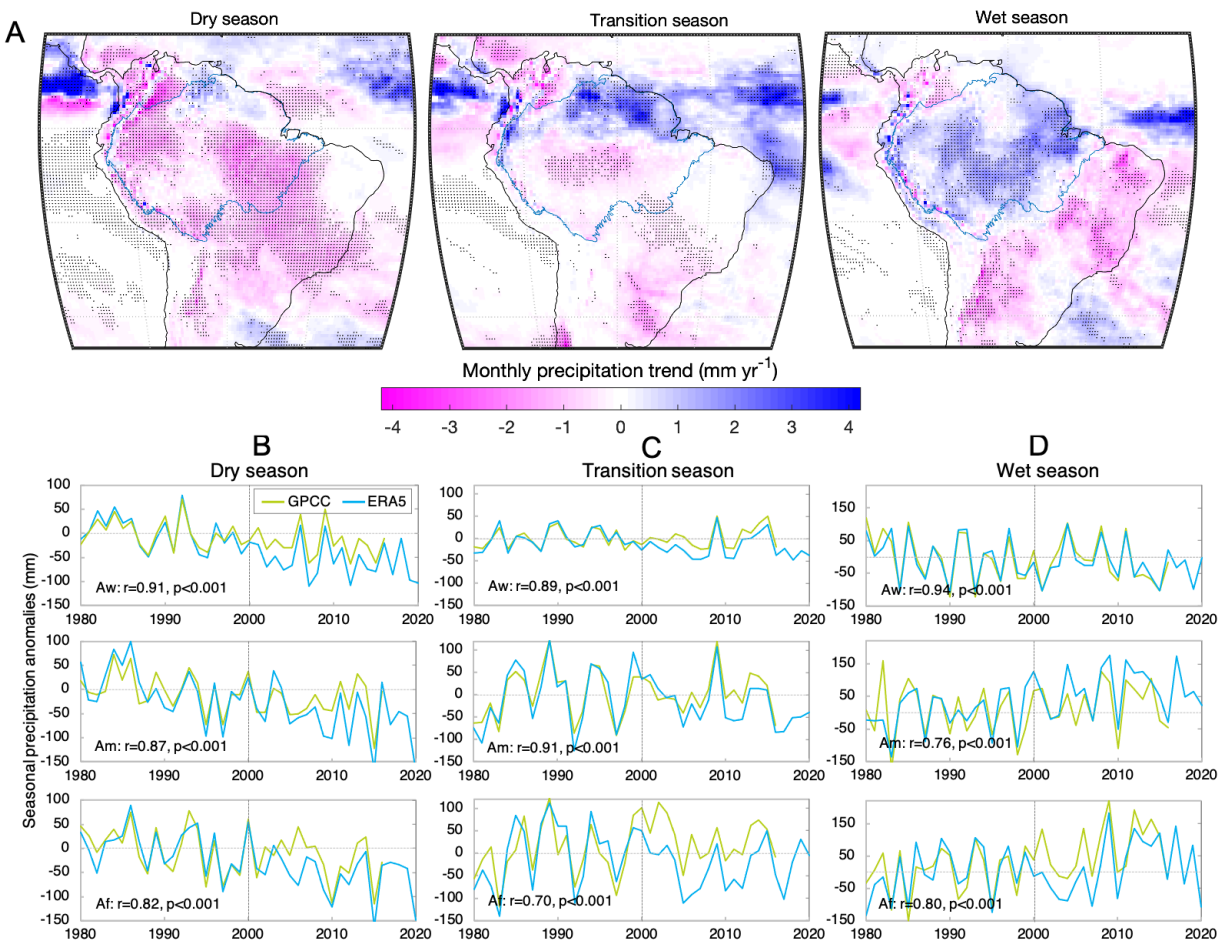

Figure. S6 Temporal changes in seasonal precipitation. Trends in monthly total precipitation (mm yr^{-1}) in the dry, transition and wet season over 1980-2019 (A), time series of precipitation anomalies (ΔP, mm) relative to the mean seasonal precipitation over 1980-1999 for (B) Dry season, (C) Transition season and (D) Wet season in tropical savanna (Aw), monsoon (Am) and rainforest (Af) climate zones. ERA5 precipitation anomalies were plotted over 1980-2020 while GPCC precipitation anomalies were plotted over 1980-2016. The dotted mask in A denotes the trend is statistically significant with $p<0.05$. *r* in B-D is the correlation between the time series of ERA5 precipitation anomalies and GPCC precipitation anomalies over their overlapping period 1980-2016.

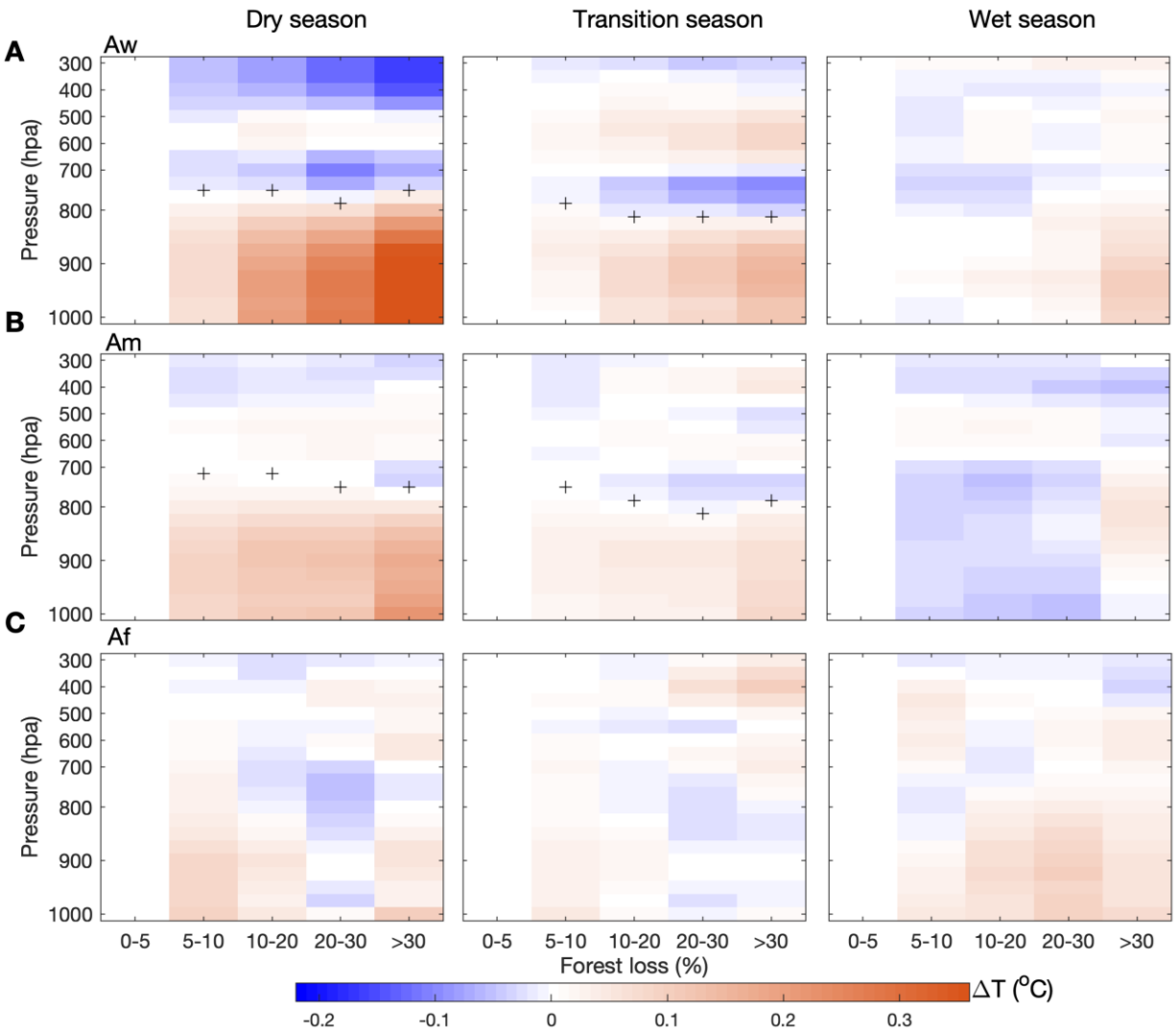

Figure. S7 Warming contribution of deforestation as a function of forest loss. The air temperature change (ΔTa, °C) profiles from 1000hpa to 300hpa in 2000–2019 in relative to 1980–1999 for tropical (A) savanna (Aw), (B) monsoon forest (Am) and (C) rainforest (Af) climate zones during the dry, transition and wet seasons contributed by deforestation. The black "+" indicate the level below which forest loss positively contributed to the warming.

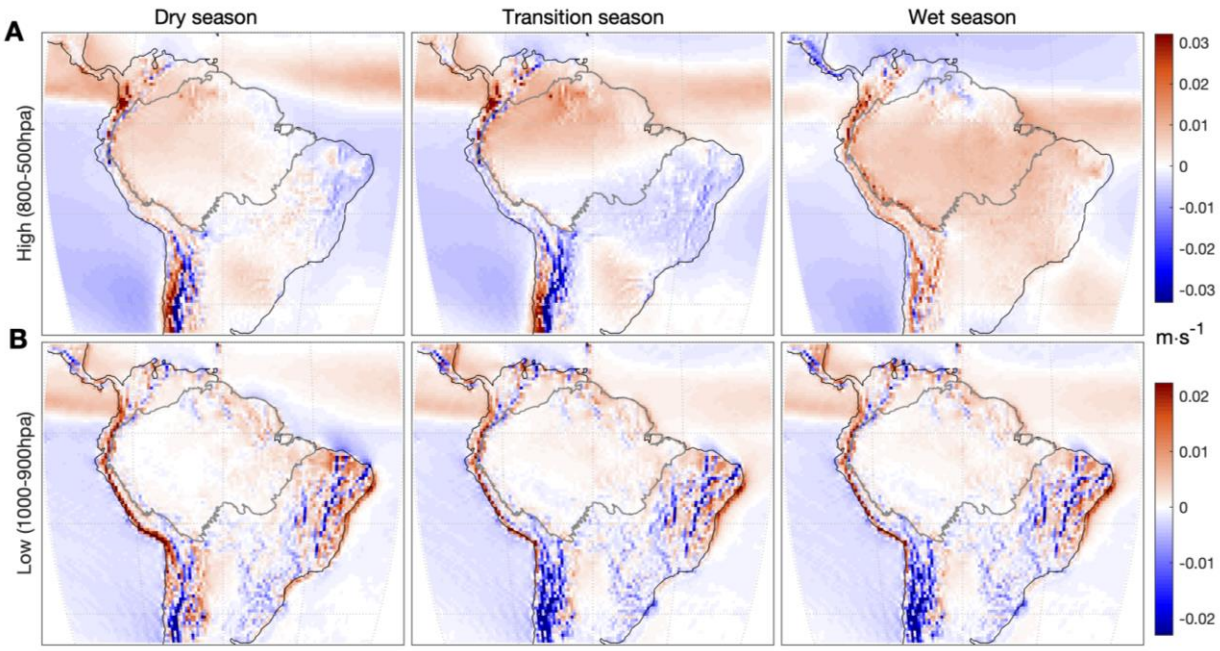

Figure. S8 The mean updraft wind velocity in the lower and middle troposphere. The mean (1980–1999) updraft wind velocity (w, ms^{-1}) in (A) the middle troposphere (500–800hpa) and (B) the lower troposphere (900–1000hpa) during the dry, transition and wet seasons.

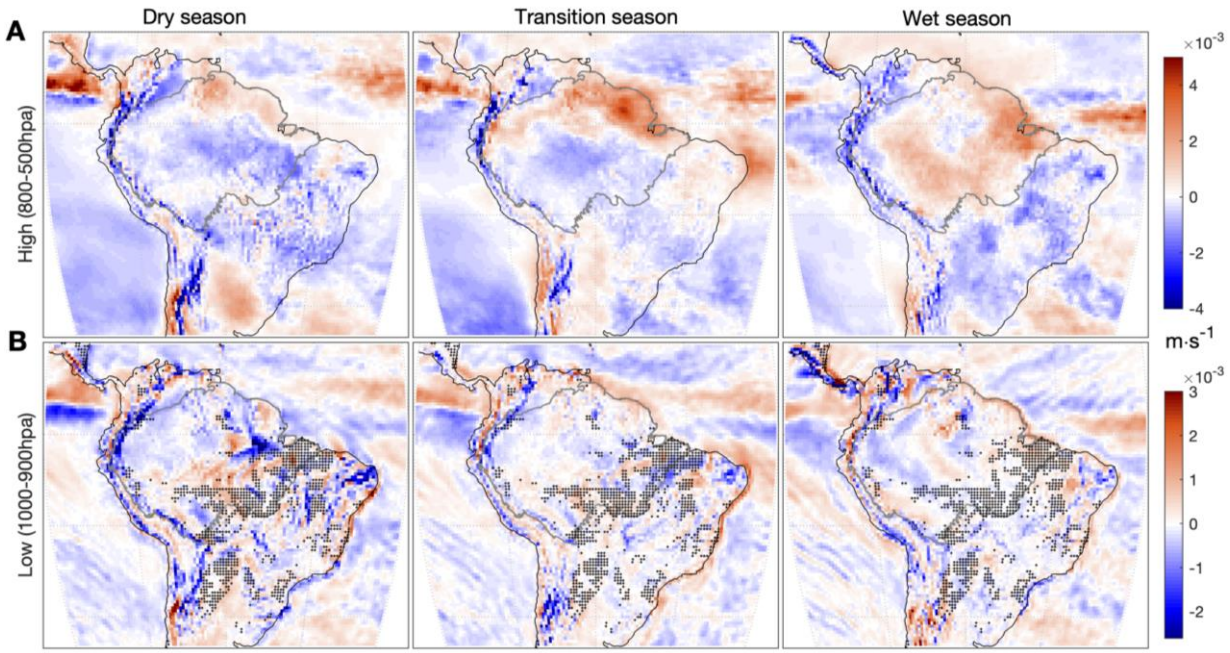

Figure. S9 The updraft wind velocity change in the lower and middle troposphere. The updraft wind velocity (*w*, ms^{-1}) change during 2000–2019 in relative to 1980–1999 in (A) the middle troposphere (800–500 hpa) and (B) lower troposphere (1000–900 hpa) in the dry, transition and wet seasons. The black "+" in (B) denotes the forest loss >10%.